J Mater Sci (2006) 41:6305–6312
DOI 10.1007/s10853-006-0492-y

Toward the preparation of a nanocomposite material through surface initiated controlled/''living'' radical polymerization of styrene inside the channels of MCM-41 silica

**Maurizio Lenarda · Gavino Chessa · Elisa Moretti ·
Stefano Polizzi · Loretta Storaro · Aldo Talon**

Received: 11 August 2004 / Accepted: 18 August 2005 /

Abstract A hybrid organic–inorganic material was prepared by surface initiated controlled/''living'' radical polymerization (CRP) of styrene in the internal space of a MCM-41 silica. The inorganic precursor was synthesized, via sol–gel, using tetraethoxysilane and cetyltrimethylammonium bromide, in the presence of ammonia and ethanol to induce the formation of submicrometric spherical particles. After characterization by powder X-ray diffraction (XRD), transmission electron micrography (TEM), scanning electron micrography (SEM), N_2 adsorption and titration of the surface silanol groups, the mesoporous silica was functionalized through a 3-step grafting process, in order to link the nitroxide initiator to the inorganic matrix (TEMPO-MCM-41). The anchorage of the TEMPO-based initiator was checked by diffuse reflectance infrared spectroscopy (DRIFT-IR). Experimental data confirmed that the styrene polymerization occurred inside the MCM-41 channels system.

Introduction

In recent years, combining organic and inorganic reagents on a nanometer/submicrometer scale, to create functional hybrid materials is receiving a great deal of attention. Organic modification of inorganic materials such as silicas and/or silicates, not only permits a precise control of surface properties for specific applications, but also can affect their bulk properties. In fact, organic features can introduce flexibility into the framework, while the inorganic components can provide structural, mechanical or thermal stability [1–6]. One of the most important class of nanocomposites are the materials obtained by the incorporation of various kind of polymers of controlled physico-chemical properties into porous inorganic material. The insertion of the polymers into the inorganic host cavities can be obtained carrying out the polymerization process inside the cavities themselves [7–15]. If the initiator is covalently bound to inner surface of the host the polymer can be synthesized directly inside the host pores [12, 15–21]. Recent developments in surface initiated ''living'' anionic and controlled ''living'' radical polymerization (CRP) [22, 23] are providing a particularly valuable ''grafting'' methodology that allows one to initiate the polymerization from functional groups tethered to the inorganic surface [10, 24–26]. The ordered mesoporous silica, known as MCM-41, was first described by Mobil researchers [27]. The material is characterized by a high specific surface area and pore volume, an ordered pore system with a hexagonal geometry and a narrow pore size distribution. The pore walls are composed of amorphous silica with an approximate thickness of about 1 nm that can be modified by changing the synthetic parameters or by

---

M. Lenarda (✉) · E. Moretti · L. Storaro · A. Talon
INSTM and Department of Chemistry, University
Ca' Foscari of Venice, Via Torino, 155/b, Mestre, Venezia
30172 (VE), Italy
e-mail: lenarda@unive.it

G. Chessa
INSTM and Department of Chemistry, University
Ca' Foscari of Venice, Calle Larga S. Marta, 2137, Venezia
30123 (VE), Italy

S. Polizzi
INSTM and Department of Physical Chemistry, University
Ca' Foscari of Venice, Via Torino, 155/b, Mestre, Venezia
30172 (VE), Italy

post-synthetic treatments. The pore size, that can range between 2 nm and 8 nm, can be adjusted during the synthesis using surfactants of different chain length or by addition of suitable organic molecules. Furthermore, a careful tuning of the synthesis parameters allows one to obtain ordered mesoporous silica particles of a well-defined shape. The synthesis of a polymer inside the pore system of a highly ordered mesoporous material appeared soon particularly interesting and it has been the subject of various studies [17–21, 28–30]. In this work we describe the preparation and the use of a TEMPO (2′,2′,6′,6′-tetramethyl-1′-piperidinyloxy)-based derivative, covalently tethered to the internal walls MCM-41 silica, to initiate the CRP of styrene. The inorganic host was prepared as spheres of submicrometric dimensions in order to have a microdimensionally more uniform material.

Experimental section

Materials

All chemicals were provided by Aldrich and used without purification, except for styrene, toluene and tetrahydrofuran, which were distilled immediately before use.

Synthetic procedures

Synthesis of 1-hydroxy-2-phenyl-2-(2′,2′,6′,6′-tetramethyl-1′-piperidinyloxy) ethane

The precursor TEMPO initiator was prepared following the conditions described in the literature (yield 92%) [31].

Preparation of the MCM-41 spheres

The spherical silica particles featuring a MCM-41 type structure were synthesized following the procedure described by Grün et al. [32] using tetraethoxysilane as silica source, cetyltrimethylammonium bromide as cationic surfactant, ethanol as the solvent and aqueous ammonia as catalyst, to allow control of the morphology during the synthesis.

Synthesis of 3-aminopropylsilylated MCM-41 (NH_2-MCM-41)

A suspension of MCM-41 silica (0.7 mmol OH/1 g) in freshly distilled toluene (30 mL) was refluxed and stirred with 3-aminopropyltriethoxysilane (0.7 mmol) for 5 h. The solid was successively filtered and washed by continuous extraction with diethyl ether and dichloromethane in a Soxhlet apparatus [33].

Synthesis of 3-amidopropylsilylated MCM-41

Triethylamine (0.7 mmol) was added to a suspension of terephtaloyl chloride (17.5 mmol) in dry carbon tetrachloride. A freshly activated (1 h at 120 °C) NH_2-MCM-41 (0.7 mmol NH_2/g) sample was slowly added to the mixture and stirred for 24 h at 0 °C.

The modified solid was filtered, washed first with carbon tetrachloride and then in a Soxhlet extractor with diethyl ether and dichloromethane.

Immobilization of 1-hydroxy-2-phenyl-2-TEMPO-ethane by bonding with the 3-amidopropylsilylated MCM-41 (TEMPO-MCM-41)

A total of 0.7 mmol of 1-hydroxy-2-phenyl-2-TEMPO-ethane was dissolved in dry tetrahydrofuran (30 ml) at room temperature. Sodium hydride 60% wt (1.05 mmol) was then added. After stirring (30 min), 3-amidopropylsilylated MCM-41 was rapidly added. The mixture was stirred under argon at room temperature for 24 h.

The solid was filtered, washed with methanol and then dried at 70 °C under vacuum.

Polymerization of styrene on TEMPO-MCM-41

Freshly activated (1 h at 120 °C) TEMPO-MCM-41 (1 mmol) and freshly distilled styrene (100 mmol) were mixed in a round-bottom flask under argon after which the mixture was heated at 125 °C under argon for 24 h [34].

The resulting material was then filtered, washed with chloroform in a Soxhlet apparatus for 9 days and dried overnight at room temperature.

Instrumental and procedures

Characterizations

^{1}H-NMR was recorded in a ($CDCl_3$) solution with a Bruker Aspect Advance 300 (300 MHz) spectrometer, considering the TMS proton signal as an internal standard.

Powder X-ray diffraction patterns were measured using a Philips diffractometer with Cu-Kα Ni-filtered radiation, a graphite monochromator and a proportional counter with a pulse height discriminator.

Adsorption–desorption experiments using N_2 were carried out at –196 °C on a Micromeritics ASAP 2010. Before each measurement the samples were outgassed first at 130 °C for 12 h at 0.67 Pa and then at room temperature for 2 h at 5.1×10^{-7} Pa. The N_2 isotherms were used to determine the specific surface areas (S.A.), using the BET equation, and the specific pore volume (V_s). V_s was calculated at $p/p° = 0.98$. The pore size distribution was calculated following the BJH method.

Scanning electron micrographs were taken on a JEOL-JSM 5600 LV microscope, equipped with a 6587 EDS (Energy Dispersive X-ray Spectrometry) detector, using an accelerating voltage of 20 kV. The samples were deposited on a sample holder with an adhesive carbon foil and sputtered with gold.

Transmission electron micrographs were taken on a JEOL-JEM 3010 high-resolution microscope (point resolution 0.14 nm), equipped with a lanthanum hexaboride (LaB_6) gun, using an accelerating voltage of 300 kV. The images were taken with a CCD camera (Gatan, mod. 694). The powder was suspended in isopropyl alcohol and dropped on a holey carbon film grid.

FT-Infrared spectra were recorded on a Nicolet Magna-IR^{TM} spectrophotometer in the 4000–400 cm^{-1} region (resolution of 4 cm^{-1}), equipped with an AVATAR 360 FT-IR E.S.P. diffuse reflectance accessory.

Determination of the number of surfae silanol groups of MCM–41 silica

Titration of silanol groups of the MCM-41 sample was carried out by a procedure analogous to that described by Van Der Voort [35].

The procedure is based on the reaction of 1,1,1,3,3,3-hexamethyldisilazane (HMDS), a selective poison for Brönsted acid sites, with the OH groups of silica [36]. The reaction yields very stable trimethylsilyl groups which are bound to the surface according to the following reaction:

$$2SiOH + (CH_3)_3SiNHSi(CH_3)_3 \rightarrow 2SiOSi(CH_3)_3 + NH_3$$

A suspension of freshly activated (1 h at 120 °C) MCM-41 silica (1 g) in HMDS (30 mL) was refluxed under argon and stirred for 3 h.

The ammonia evolved during the reaction was bubbled in a set volume of H_3BO_3 0.05% (wt/wt) in water solution and the resulting solution was titrated with HCl 0.01 M.

Results and discussion

Synthesis

The synthetic strategy we have developed to attach latent TEMPO-based initiating groups to MCM-41 particles is centered on the stepwise modification of this material.

The synthesis starts by grafting 3-aminopropyl groups on the silanol-containing surface **1** to yield the aminopropyl silica, according to a literature methodology [33] (Scheme 1). Compound **2** was then reacted with terephtaloyl chloride to give the corresponding amide **3**. A large excess of terephtaloyl chloride was used in order to ensure the complete reaction of the amino groups and to minimize the formation of cross-links by reaction at both extremities of the diacid chloride. After purification using the standard protocol described in the Experimental Section, the modified silica 3 was treated with 1-hydroxy-2-phenyl-2-(2′,2′,6′,6′-tetramethyl-1′-piperidinyloxy)ethane to affo rd the desired material **4**.

The most important feature of these TEMPO-based initiators is the presence of a homolitically unstable alkoxyamine (C–ON) bond. This permits, during polymerization, reversible homolysis of the covalent species, followed by monomer insertion and reversible recombination [37, 38] (Scheme 2). The presence of inactive chain ends results in a dramatic reduction of the concentration of radical chain ends which coupled with the inability of the nitroxide free radicals to initiate new chain growth, leads to a lower number of unwanted side reactions (termination, combination or disproportionation).

Structural and morphological characterization of the silica microspheres

The XRD pattern of the mesoporous material is shown in Fig. 1. The observation of several Bragg peaks at low reflection angles (2.5–7.0° 2θ), which can be indexed in a hexagonal lattice and correspond well to the hexagonally arranged pore structure of MCM-41, is the proof of a long-range order and consequently of the good quality of the sample. As the material is not crystalline at the atomic level, no reflections at higher angles are observed.

The nitrogen adsorption–desorption isotherm exhibits both a reversible type IV isotherm and a sharp pore filling step at p/p_0 0.2–0.3 which are characteristic of uniform pores (Fig. 2). The sample shows high specific surface area, approximately 1,000 $m^2\,g^{-1}$, and a

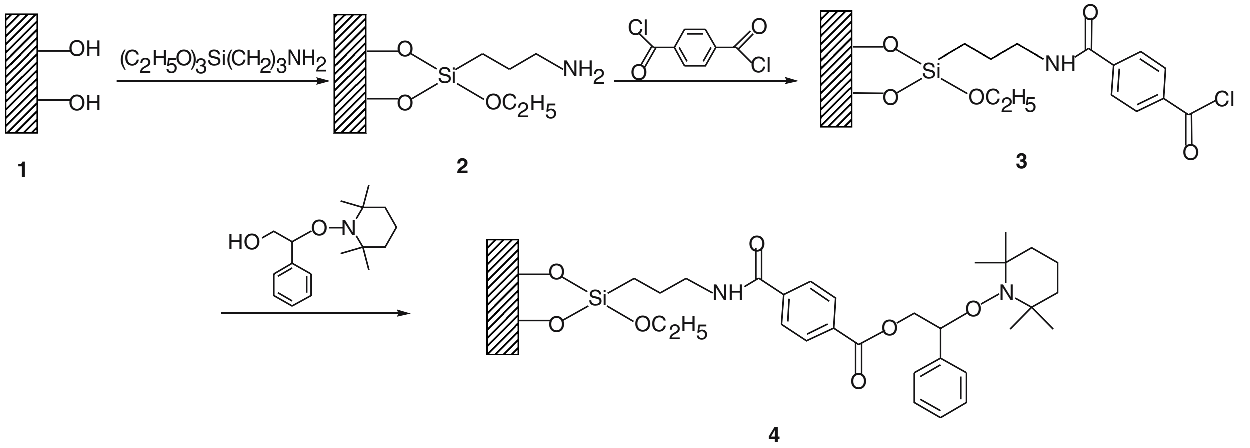

Scheme 1 Schematic representation of functionalization of MCM-41 silica

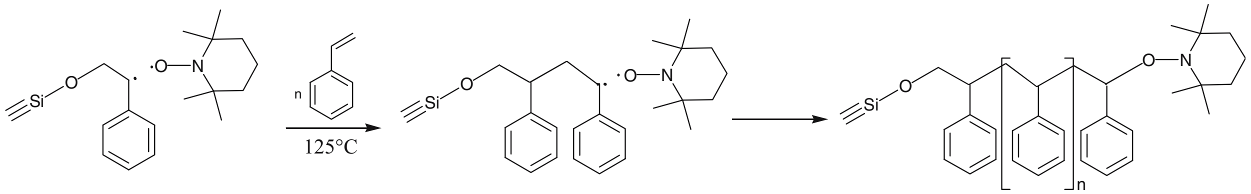

Scheme 2 Schematic representation of polymerization of styrene on MCM-41 spherical particles

narrow distribution of pore diameters centered at 2.6 nm (Table 1).

The ordered channel system can be clearly observed in the TEM micrograph (Fig. 3). The silica microspheres show a pseudo-periodic lattice of pores in the central part and a radial arrangement at the side. The images further suggest that radial parallel pore bindles start from the central part and run up to the surface of the particle, as suggested by Van Tendeloo [39].

SEM was used to confirm particle morphology and size; they resulted almost perfectly spherical, with an average size of 600 nm (Fig. 4) [40].

In conclusion, the spherical particles appear to have the same physical properties as the MCM-41 silicas synthesized by traditional methods [41–43].

Finally, the mesoporous silica was titrated following the Van Der Voort procedure and an average value of 0.7 mmol OH/g of silica was found (Table 1).

Physico-chemical characterization of the chemically modified silica spheres and of the resulting nanocomposite

All post-synthesis modifications of the mesoporous silica spheres were monitored by DRIFT-IR spectroscopy.

As shown in Fig. 5 the FT-IR spectrum of pure MCM-41 silica exhibits a broad band located in the 3,700–2,700 cm^{-1} interval, assigned to hydrogen-bonded Si–OH groups with adsorbed water. Bands ranging from 1,400 to 400 cm^{-1} arise from fundamental lattice vibrations.

The spectrum of NH_2-MCM–41 shows four further bands: two at 2,937 cm^{-1} and 2,875 cm^{-1}, characteristic of asymmetrical and symmetrical vibrations of the $–CH_2$ groups of the propyl chains and two at 3,370 cm^{-1} and 3,303 cm^{-1} that can be assigned to the NH stretching of $–NH_2$ groups.

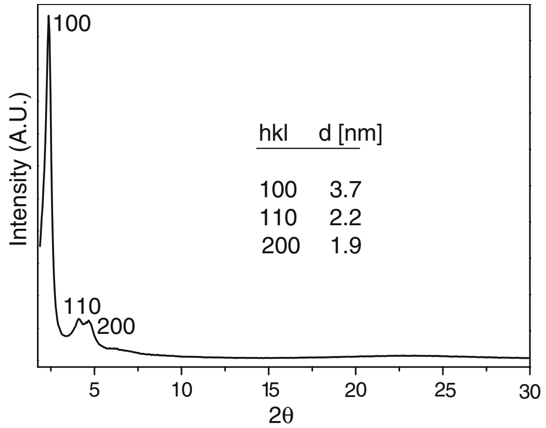

Fig. 1 X-ray diffraction pattern of freshly calcined MCM-41 spherical particles

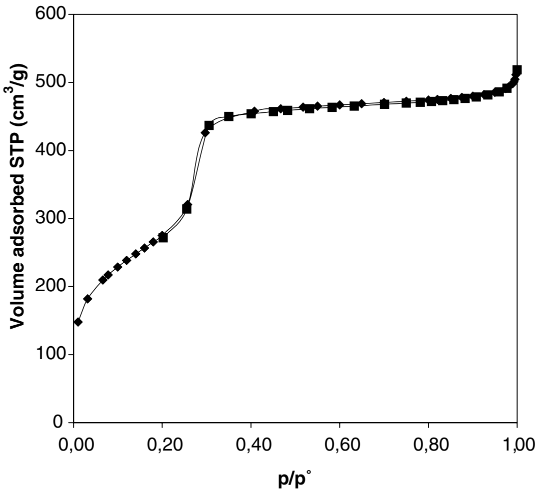

Fig. 2 N_2 sorption isotherm of MCM-41 sample (■: adsorption branch, ♦: desorption branch)

The spectrum of the amidopropylsilylated MCM-41 sample shows two bands at 1,637 cm^{-1}and 1,538 cm^{-1} that are characteristic of the amide function, and a band at 1,787 cm^{-1} that can be assigned to the carbonyl of the acid halide C=O, unambiguously indicating that the initiator is bound to the phenyl ring via an estereal bond.

The final TEMPO-MCM-41 sample shows a band at 1,712 cm^{-1}, that can be assigned to the ester carbonyl group, while the adsorption of the acylic C=O band disappears.

The FT-IR spectrum of the material, after polymerization, shows additional bands at 3,090–3,000 cm^{-1} that can be ascribed to the styrene phenyl groups (Fig. 5).

Therefore, infrared spectroscopy suggests that styrene was effectively polymerized on the surface of silica support, but it cannot be taken as an evidence of the occurrence of the reaction inside the pores. The modification of the silica pores volume after polymerization was evaluated by nitrogen adsorption and desorption measurements.

The BET value of an accurately washed with dichloromethane sample evidenced a dramatic decrease in the surface area (from 997 m^2/g to 20 m^2/g) after polymerization suggesting that 98% of the pore volume has become inaccessible to the probe molecule. The nanocomposite was calcined at 550 °C in air in order to eliminate the polymer and a BET value of 641 m^2/g was restored. The incomplete restoring of the original surface area value can be due to a partial collapse of the inorganic porous structure of the material, as a consequence of the occurrence of hot spots with temperatures much higher than 550 °C inside the porous system, as is well known to occur during the regeneration process of industrial porous catalysts and was observed studying alkanes oxidation [44] on porous catalysts. But it can also be due to a partial degradation of the polymer to non-volatile carbonaceous products that remain trapped in the most internal part of the pores system.

On the other hand, this behavior can be taken as an evidence of the effective formation of the polymer inside the cavities of the inorganic substrate.

TG and DTG patterns of the MCM-41 material and of its post-synthesis modifications are shown in Fig. 6. Comparison of the DTG profile of the MCM-41 silica (curve a) with that of calcinated at 550 °C polystyrene-MCM-41 (curve d) evidenced their close similarity, suggesting that the thermal treatment of the composite completely eliminates the included polymer and that the resulting silica is morphologically and structurally almost identical to the silica spheres before the styrene polymerization (Fig. 6).

Furthermore, the XRD pattern of the nanocomposite is similar to that of the silica sample before styrene polymerization (Fig. 7).

As shown in Fig. 7, the intensity of the peaks decreases, but their pattern is conserved, confirming that the hexagonal arrangement is retained. Therefore we can infer that the observed decrease of the surface area in the nanocomposite is the result of the polymer formation inside the silica pores. The conservation of the hexagonal arrangement after polymerization was further confirmed by TEM micrographs (Fig. 8).

On the basis of the TG/DTG data, the weight fraction of polystyrene inside the MCM-41 silica, that cannot be removed even after repeated washings, was evaluated to be 14% of the total weight. This value indicates, assuming a value of polystyrene density of

Table 1 Summary of textural characteristics of the MCM-41 sample

Sample	S.A. (m^2 g^{-1})	V_s (cm^3 g^{-1})	δ (nm)	BJH pore diameter (nm)	XRD d_{100} diameter (nm)	–OH groups (mmol g^{-1})
MCM-41	997	0.76	1.7	2.6	3.7	0.7

S.A. = B.E.T specific surface area; V_s = pore specific volume at p/p° = 0.98; δ = pore wall thickness

d_{100} = interplanar distance

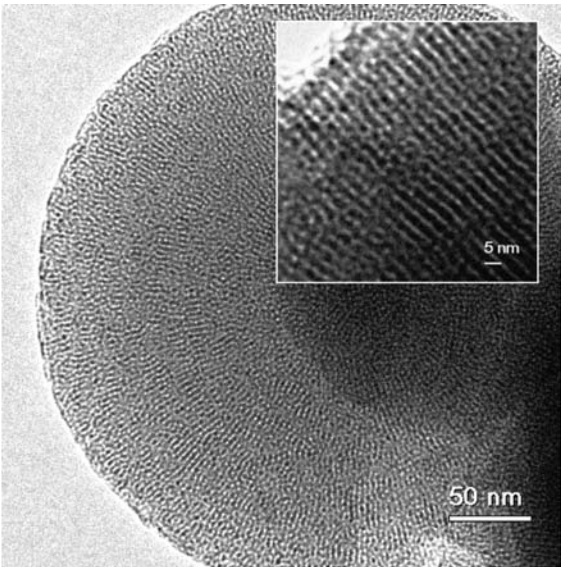

Fig. 3 Transmission electron micrograph (TEM) of MCM-41 spheres

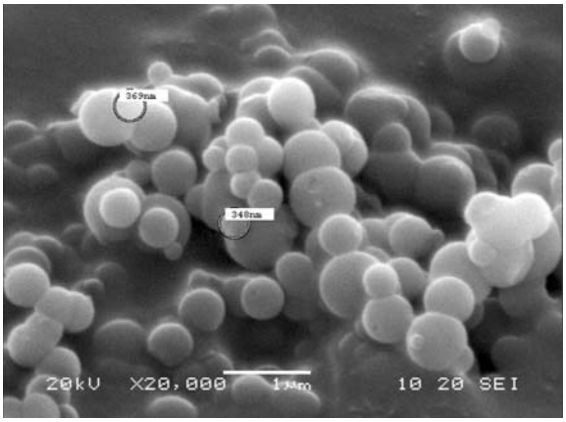

Fig. 4 Scanning electron micrograph (SEM) of MCM-41 spherical particles

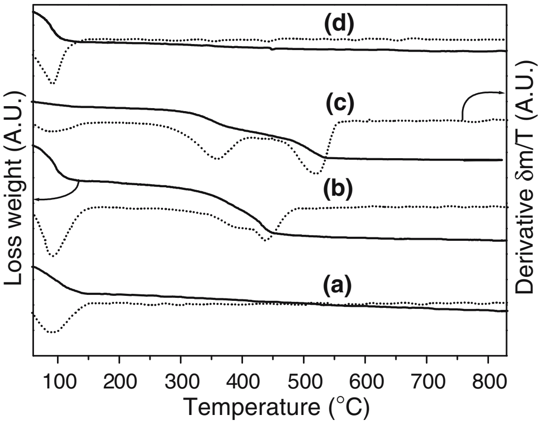

Fig. 6 Thermogravimetry and differential thermogravimetry of (**a**) MCM-41 silica; (**b**) TEMPO-MCM-41; (**c**) polystyrene-MCM-41; (**d**) polystyrene-MCM-41 after calcinations at 550 °C

1,050 kg/m^3 that at least the 30% of the silica space is filled. However, this evaluation is hazardous since it is difficult to estimate a realistic value for the density because the polymerization process and consequently the polymer final structure is conditioned by the MCM-41 chemical and framework properties, with a likely effect on the packing efficiency. Nitrogen physisorption gives an estimate of the surface accessible to the probe molecule. A partial occlusion of the pores, like that caused by styrene polymerization initiated close to the pores entrance, can deeply affect the inorganic host accessibility to the nitrogen molecules. On the other hand, TG/DTG determinations give the total amount of organic matter occluded in the inorganic host, thus, it's quite probable that more than the above calculated volumes are filled with polystyrene in these composites.

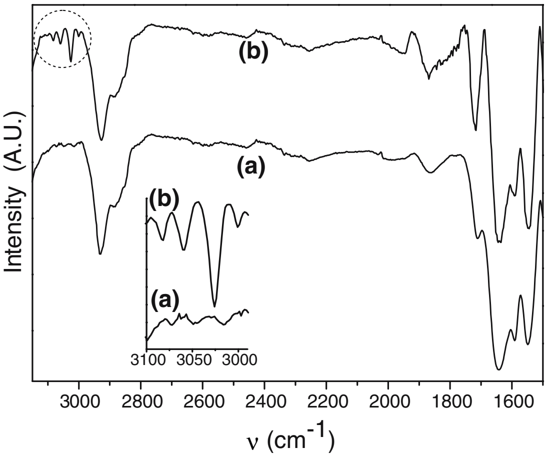

Fig. 5 DRIFT-IR spectrum of MCM-41 silica (**a**) before and (**b**) after polymerization of styrene

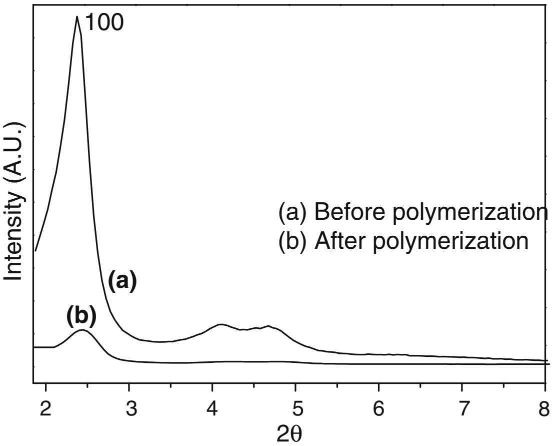

Fig. 7 XRD patterns of MCM-41 silica (**a**) before and (**b**) after polymerization

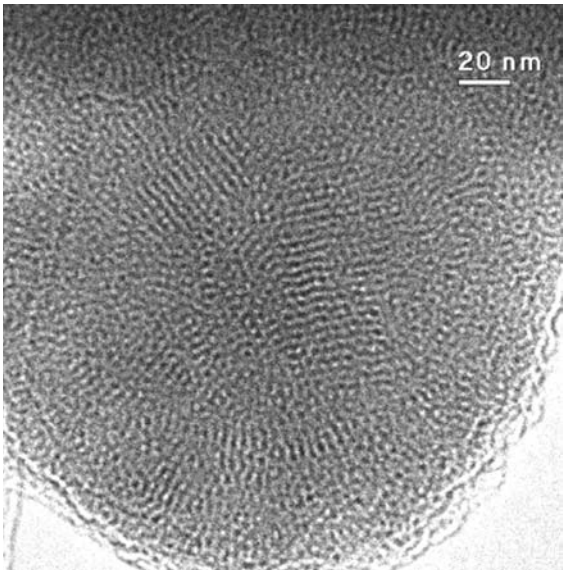

Fig. 8 Transmission electron micrograph of MCM-41 sample after styrene polymerization

Conclusions

We can conclude that styrene polymerization, initiated by a TEMPO-based system anchored to the internal surface of a modified MCM-41 silica, leads to the formation of a nanocomposite material. The partial filling of the pores, evidenced by the dramatic decrease of the surface area, occurs while retaining the structural and morphological characteristics of the starting silica. This polymerization procedure appears suitable to insert polystyrenic frameworks in the internal space of a structurally ordered porous inorganic material. In this context it would be particularly interesting that the incorporation of functionalized polystyrenes in this kind of structurally ordered inorganic hosts and studies are in progress on these topics.

Acknowledgment Financial support from the MIUR (Ministero dell'Istruzione, Università e Ricerca) is gratefully acknowledged.

References

1. Mark JE, Lee CY, Bianconi PA (1995) Hybrid inorganic. Organic composites, vol 585. American Chemical Society, Washington, DC
2. Stein A, Melde BJ, Schroden RC (2001) Adv Mater 12:1403
3. Anwander R (2001) Chem Mater 13:4419
4. De Vos DE, Dams M, Sels BF, Jacobs PA (2002) Chem Rev 102:3615
5. Tao T, Maciel GE (2000) J Am Chem Soc 122:3118
6. Sayari A, Hamoudi S (2001) Chem Mater 13:3151
7. Cardin DJ (2002) Adv Mater 14:553
8. Schmidt D, Shah D, Giannelis EP (2002) Curr Opin Solid State Mater Chem 6:205
9. Frisch HL, Mark JE (1996) Chem Mater 8:1735
10. Pyun J, Matyjaszewski K (2001) Chem Mater 13:3436
11. Manias E, Touny A, Wu L, Strawhecker K, Lu B, Chung TC (2001) Chem Mater 13:3516
12. Weckhuysen BM, Ramachandra Rao R, Pelgrims J, Schoonheydt RA, Bodart P, Debras G, Collart O, Van der Voort P, Vansant EF (2000) Chem Eur J 6:2960
13. Spange S, Gräser A, Huwe A, Kremer F, Tintemann C, Behrens P (2001) Chem Eur J 7:3722
14. Tajima K, Aida T (2000) Chem Commun 2399
15. Spange S, Gräser A, Müller H, Zimmermann Y, Rehak P, Jäger C, Fuess H, Baehtz C (2001) Chem Mater 13:3698
16. Kageyama KK, Tamazawa J, Aida T (1999) Science 285:2113
17. He J, Duan X, Evans DG, Howe RF (2002) J Porous Mat 9:49
18. Tudor J, O'hare D (1997) Chem Commun 8:603
19. Johnson SA, Khushalani D, Coombs N, Mallouk TE, Ozin GA (1998) J Mater Chem 8:13
20. Kageyama K, Ogino S, Aida T, Tatsumi T (1998) Macromolecules 31:4069
21. Rahiala H, Beurroies I, Eklund T, Hakala K, Gougeon R, Trens P, Rosenholm JB (1999) J Catal 188:14
22. Patten TE, Matyjaszewski K (1998) Adv Mater 10:902
23. Chessa G, Scrivanti A, Matteoli U, Castelvetro V (2001) Polymer 42:9347
24. Husseman M, Malmström EE, Mc Namara M, Mate M, Mecerreyes D, Benoit DG, Hedrick JL, Mansky P, Huang E, Russell TP, Hawker CJ (1999) Macromolecules 32:1424
25. Zhou Q, Fan X, Xia C, Mays J, Advincula R (2001) Chem Mater 13:2465
26. Zhou Q, Wang S, Fan X, Advincula R (2002) Langmuir 18:3324
27. Beck JS, Vartuli JC, Roth WJ, Leonowicz ME, Kresge CT, Schmitt KD, Chu C, Olson DH, Sheppard EW, McCullen SB, Higgins JB, Shenkler JL (1992) J Am Chem Soc 114:10834
28. Moller K, Bein T, Fischer RX (1998) Chem Mater 10:1841
29. Moller K, Bein T (1998) Chem Mater 10:2950
30. Anwander R, Nagl I, Zapilko C, Widenmeyer M (2003) Tetrahedron 59:10567
31. Hawker CJ, Barclay GG, Orellana A, Dao J, Devonport W (1996) Macromolecules 29:5245
32. Grün M, Lauer I, Unger KK (1997) Adv Mater 9:254
33. Laspéras M, Llorett T, Chaves L, Rodriguez I, Cauvel A, Brunel D (1997) Stud Surf Sci Catal 108:75
34. Malmström E, Miller RD, Hawker CJ (1997) Tetrahedron 53:15225
35. Van Der Voort P (1993) Chemical surface coating – a new route towards silicon nitride coatings on silica gel. Ph.D. thesis, University of Antwerp, Antwerp
36. Vansant EF, Van Der Voort P, Vrancken KC (1995) Characterization and chemical modification of the silica surface in Stud. Surf. Sci. and Catal., vol 93. Elsevier Science Publishers, Amsterdam

37. Hawker CJ (1997) Acc Chem Res 30:373
38. Hawker CJ (1994) J Am Chem Soc 116:11185
39. Van Tendeloo G, Geuens P, Colomer JF, Lebedev OJ (2003) In: 6th multinational congress on microscopy – European exstension, Pula 2003
40. Grün M, Unger KK, Matsumoto A, Tsutsumi K (1999) Micropor Mesopor Mater 27:207
41. Kresge CT, Leonowicz ME, Roth WJ, Vartuli JC, Beck JS (1992) Nature 359:710
42. Monnier A, Schutz F, Huo Q, Kumar D, Margolese D, Maxwell RS, Stucky GD, Krichnamurty M, Petroff P, Firouzi A, Janicke M, Chmelka BF (1993) Science 261:1299
43. Hou Q, Margolese D, Ciesla U, Demuth DG, Feng P, Gier TE, Sieger P, Firouzi A, Chmelka BF, Schuth F, Stucky GD (1994) Nature 368:317
44. Basile F, Fornasari G, Trifiro' F, Vaccari A (2001) Catal Today 64:21